Molecular dynamics simulation studies of the influence of imidazolium structure on the properties of imidazolium/azide ionic liquids

Justin B. Hooper, Oleg N. Starovoytov, Oleg Borodin, Dmitry Bedrov, and Grant D. Smith

Citation: J. Chem. Phys. **136**, 194506 (2012); doi: 10.1063/1.4718800
View online: http://dx.doi.org/10.1063/1.4718800
View Table of Contents: http://jcp.aip.org/resource/1/JCPSA6/v136/i19
Published by the American Institute of Physics.

Molecular dynamics simulation studies of the influence of imidazolium structure on the properties of imidazolium/azide ionic liquids

Justin B. Hooper,[1,a)] Oleg N. Starovoytov,[2] Oleg Borodin,[3] Dmitry Bedrov,[2] and Grant D. Smith[1]
[1]*Wasatch Molecular Inc., 825 N. 300 W. Ste. W003, Salt Lake City, Utah 84103, USA*
[2]*Department of Materials Science and Engineering, University of Utah, Salt Lake City, Utah 84112, USA*
[3]*Electrochemistry Branch, Army Research Laboratory, 2800 Powder Mill Rd., Adelphi, Maryland 20783, USA*

(Received 15 November 2011; accepted 2 May 2012; published online 18 May 2012)

Atomistic molecular dynamics simulations were performed on 1-butyl-3-methyl-imidazolium azide [bmim][N_3], 1-butyl-2,3-dimethylimidazolium azide [bmmim][N_3], and 1-butynyl-3-methyl-imidazolium azide [bumim][N_3] ionic liquids. The many-body polarizable APPLE&P force field was augmented with parameters for the azide anion and the bumim cation. Good agreement between the experimentally determined and simulated crystal structure of [bumim][N_3] as well as the liquid-state density and ionic conductivity of [bmmim][N_3] were found. Methylation of bmim (yielding bmmim) resulted in dramatic changes in ion structuring in the liquid and slowing of ion motion. Conversely, replacing the butyl group of bmim with the smaller 2-butynyl group resulted in an increase of ion dynamics. © *2012 American Institute of Physics*. [http://dx.doi.org/10.1063/1.4718800]

I. INTRODUCTION

Ionic liquids (ILs) containing azide anions are being explored as energetic materials and as candidates for hypergolic fuel applications.[1,2] Variations in chemical structure of ions are often considered as a route to obtain optimal thermophysical properties for desired applications. Therefore understanding of how these modifications correlate with structural, thermodynamic, and transport properties of ILs is an important aspect in the design and selection of an optimal IL. In this manuscript we extend our previously developed many-body polarizable APPLE&P force field[3] to include the azide anion as well as the 1-butynyl-3-methyl-imidazolium cation. We utilize the developed potential in molecular dynamics (MD) simulation studies of the influence of cation structure on imidazolium-based azide ILs and provide comparison of simulation results utilizing this force field with available experimental data on imidazolium-azide ILs.

II. FORCE FIELD DEVELOPMENT

The 1-butyl-3-methyl-imidazolium (bmim), 1-butyl-2,3-dimethylimidazolium (bmmim), and 1-butynyl-3-methyl-imidazolium (bumim) cations investigated in this work as well as the azide anion (N_3^-) are illustrated in Figure 1. We utilize the Atomistic Polarizable Potential for Liquids, Electrolytes, and Polymers (APPLE&P)[3] as a starting point for the development of the force field for azide-based ILs since previous MD simulations utilizing the APPLE&P force field have yielded accurate predictions of density, heat of vaporization, ion self-diffusion coefficients, conductivity and viscosity for numerous ILs.[3–6] For this work, we have extended APPLE&P by adding parameters for N_3^- and bumim.

The methodology employed for parameterization of the force field follows the general procedures outlined in our previous work.[3] Partial charges for N_3^- and bumim were fit to the electrostatic potential derived from *ab initio* calculations utilizing GAUSSIAN09[7] at the MP2/cc-pvTz (MP2/aug-cc-pvDz) level for the N_3^- (bumim), with the electrostatic potential discretized onto a grid of 80 000 points around the respective ions. Atomic polarizabilities for N_3^- were fit by adjusting atomic polarizabilities to reproduce both the total molecular polarizability as well as a series of binding energies generated via *ab initio* calculation of the interaction of a +0.5e test charge with the anion at the MP2/cc-pvTz level of theory. Atomic polarizabilities for bumim were transferred from the previously developed APPLE&P parameters for the constituent atoms represented in bmim and 2-butyne as appropriate. Repulsion/dispersion parameters for nitrogen atoms in N_3^- were fit by matching the density and enthalpy of vaporization to experimental data[8] for 1-azidobutane, yielding estimates within 1% of experimental values. All other repulsion/dispersion parameters were transferred from previously established values present in APPLE&P.[3]

Dihedral parameters for the C-N-C-C torsion (see Fig. 1) linking the butynyl group to the imidazolium heterocycle of the bumim cation were fit to the energies from *ab initio* calculations obtained at the MP2/aug-cc-pvDz level, as shown in Figure 2. In order to better understand the effect of conformational interconversion on the dynamics of the [bumim][N_3] we have also implemented a modified dihedral potential denoted as [bumim-mod], which increases the dihedral barrier by 2 kcal/mol as shown in Figure 2. Force field parameters for the extended version of APPLE&P can be obtained from Wasatch Molecular, Inc.[9]

a)Author to whom correspondence should be addressed. Electronic-mail: jbhooper@wasatchmolecular.com.

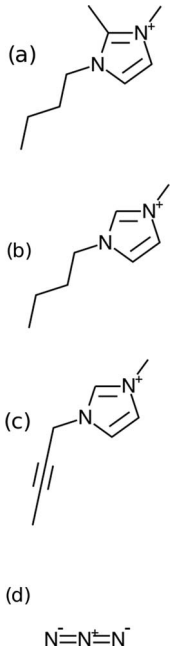

FIG. 1. (a) 1-butyl-2,3-dimethylimidazolium, (b) 1-butyl-3-methylimidazolium, (c) 1-butynyl-3-methylimidazolium, and (d) azide anion.

III. MOLECULAR DYNAMICS SIMULATION METHODOLOGY

Cubic simulation cells with 3-D periodic boundary conditions for [bmim][N_3], [bmmim][N_3], and [bumim][N_3] were comprised of 150 ionic pairs. MD simulations were carried out using the simulation package Lucretius.[10] The velocity Verlet form of the SHAKE algorithm[11] was employed to constrain the bond lengths. The Ewald summation method was used for electrostatic interactions between partial charges. Partial charge interactions between atoms separated by three bonds were reduced by 80%. Thole screening[12] was utilized to avoid the "polarization catastrophe," with the Thole parameter set to 0.2. Multiple timestep integration[13] with an inner timestep of 0.5 fs (harmonic bending contributions), a central time step of 2.0 fs (torsional contributions; nonbonded interactions within a radius of 7.0 Å) and an outer timestep of 4.0 fs (nonbonded interactions between 7.0 Å and 10.5 Å, the reciprocal contribution of the Ewald summation, and direct dipole-dipole induced polarization) was employed. An iterative scheme was employed to calculate induced dipole-induced dipole interactions. A cubic damping function is employed to ensure a continuous polarization potential starting at 9.5 Å and reaching zero by the full cutoff radius of 10.5 Å. Pressure and temperature control in NVT and NPT ensemble simulations were implemented using the integration scheme proposed by Martyna *et al.*[13] with frequencies of 0.01 fs^{-1} and 0.005 fs^{-1} for the thermostat and barostat control.

All ILs were initially set up with random ion placement at low density followed by compression of simulation boxes until liquid densities were obtained at 393 K. Equilibration of all systems at 393 K was performed over a 2 nanosecond (ns) period via isobaric-isothermal (NPT) ensemble simulation. A stepwise cooling approach was carried out to obtain lower temperatures. Further equilibration runs were performed at production temperatures of 333 K, 348 K, 363 K, and 393 K of between 6 ns and 15 ns, until the density of the liquids stabilized. Following this, canonical (NVT) ensemble simulation was employed for production of 10 ns trajectories.

For the simulation of the [bumim][N_3] crystal the system was comprised of 96 ionic pairs arranged in a 4 × 3 × 4 supercell. A mixed Monte Carlo/molecular dynamics (MC/MD) simulation technique was used for crystal simulation,[14,15] with an MD segment represented by NVT ensemble MD simulation for 2 ps with the same integrator parameters as described above, while an MC segment is represented by a series of 10 individual attempts to perturb the lattice vectors and angles of the crystalline supercell with center-of-mass rescaling of the simulated molecules to reflect the new supercell. The combination of such an MD segment and MC segment combines to form a single iteration. Equilibration was initially carried out with 100 iterations, after which the production run commenced at 173 K with a length of 10 ns.

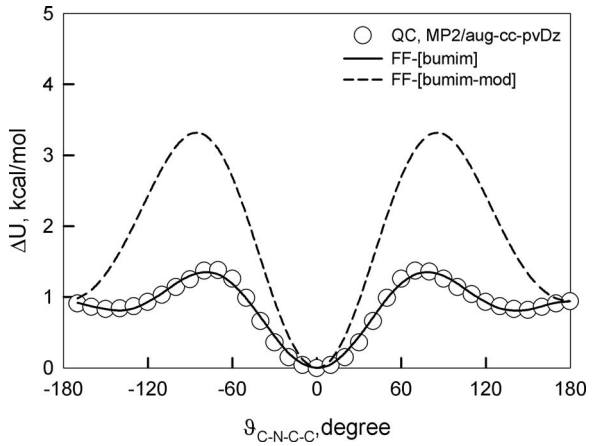

FIG. 2. Conformational energy for the C-N-C-C torsion of the 2-butynyl side chain in bumim calculated at MP2/aug-cc-pvDz and from the developed force field (solid line). Short dashed line indicates an artificially increased dihedral barrier for bumim by about 2 kcal yielding the [bumim-mod] cation.

IV. SIMULATION RESULTS

A. Crystal structure of [bumim][N_3]

A comparison of the lattice parameters of [bumim][N_3] obtained from x-ray measurements[16] with simulations is shown in Table I. Good agreement between the simulation and experiment can be seen with deviations for individual cell parameters varying between 1% and 4%, while the unit cell volume is within 1.5% of the experimental value.

B. Cation volumes and ionic liquid density

Based upon simulation densities at 333 K, the volume of the [bumim][N_3] ion pair is estimated to be 261 $Å^3$, while the corresponding volumes of [bmim][N_3] and [bmmim][N_3] ion pairs are 286.7 $Å^3$ and 309.3 $Å^3$ respectively. Thus, we approximate that [bmmim] has a volume 22.6 $Å^3$ larger than [bmim], while [bumim] has a volume 25.7 $Å^3$ smaller

TABLE I. Comparison of simulated vs. experimental values for [bumim][N_3] crystal parameters at 173 K.

Parameter	Simulated (Experiment (Ref. 16))	Deviation, %
a (Å)	7.52 (7.195)	+4.5
b (Å)	8.15 (8.238)	− 1.0
c (Å)	8.51 (8.447)	+0.8
α (°)	66.9 (68.765)	− 2.7
β (°)	89.0 (89.253)	− 0.3
γ (°)	77.0 (80.307)	− 4.1
Density (g/cm^3)	1.262 (1.281)	− 1.5
Unit cell volume (Å^3)	466.3 (459.4)	+1.5

than [bmim]. The predicted azide-based IL densities are given in Figure 3 as a function of temperature. Densities for [bmmim][N_3] agree well with experiment.[17] The densities of [bmmim][N_3] and [bmim][N_3] are very similar, while the density of [bumim][N_3] is greater than these by about 10%. These results are well correlated with the size of the cations, with the smallest cation yielding the highest density IL. We also studied the influence of the dihedral barrier on densities of [bumim][N_3]. Increasing the rotational barrier by ~2 kcal/mol did not affect the density at the simulated temperatures.

C. Ion self-diffusion

Ion self-diffusion coefficients $D_\pm$ were calculated using the Einstein relation:

$$D_\pm = \lim_{t\to\infty} \frac{MSD(t)}{6t}, \quad (1)$$

where MSD(t) is the squared ion center-of-mass displacement averaged over all ions of the same charge and multiple time origins after time t. The diffusion coefficient was calculated by fitting MSD(t) to the linear equation a*t + c in the diffusive regime. A correction for the finite size of the simulation box to the diffusion coefficient[18] was estimated to be about 10% based on similar simulations of related ILs[3] and was applied to the self-diffusion coefficient for all ILs at all temperatures.

The cation and anion self-diffusion coefficients are given in Figures 4(a) and 4(b). The ion self-diffusion coefficients exhibit the following behavior: [bumim][N_3] > [bmim][N_3] > [bmmim][N_3]. The difference between cation self-diffusion coefficients is more pronounced compared to the difference of anion self-diffusion coefficients as expected because the cation chemical structure is varied while the structure of the anion is fixed. The order of ion self-diffusion coefficients correlates well with the size of the cation (see Table II).

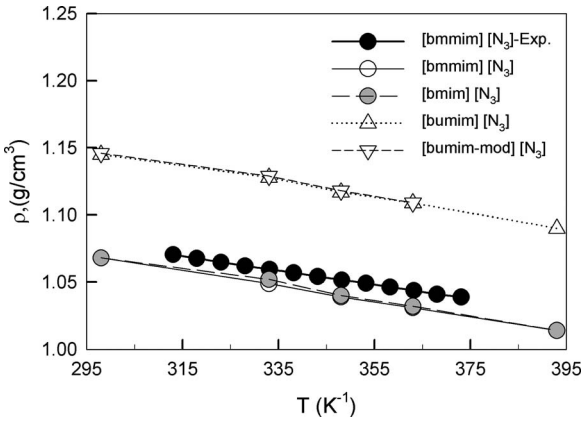

FIG. 3. Ionic liquid density as a function of temperature. Experimental data are taken from Ref. 17.

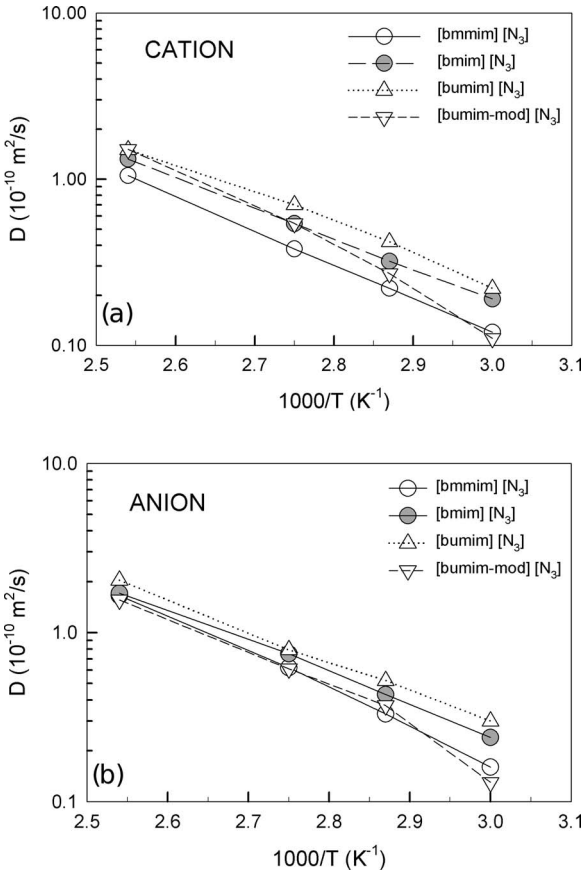

FIG. 4. Ion self-diffusion coefficients as a function of inverse temperature are given for cations (a) and anions (b) as obtained from MD simulations.

The influence of the conformation transition barrier of the 2-butynyl group on ion diffusion in [bumim][N_3] was also investigated. Increasing the torsional barrier by 2 kcal/mol hinders dihedral relaxation by a factor of five at 333 K while slowing ion transport noticeably but to a smaller extent as shown in Figures 4(a) and 4(b). Interestingly, increasing the dihedral barrier for the 2-butynyl group slows down ion diffusion by about the same amount as changing from a butyl side group to the smaller 2-butynyl increases ion diffusion. Hence,

TABLE II. Enthalpy of vaporization and mean ion self-diffusion coefficients for azide ionic liquids at 333 K.

Cation	D_+ ($\times 10^{-10}$), m^2/s	D_- ($\times 10^{-10}$), m^2/s	ΔH_{vap}, kJ/mol
bmim (0.0)[a]	0.19	0.25	155.0
bmmim (22.6)[a]	0.12	0.17	142.6
bumim (−25.7)[a]	0.21	0.29	158.2
bumim_mod (−25.7)[a]	0.10	0.14	158.1

[a]Estimated cation volume relative to bmim (Å^3).

ion diffusion in [bumim-mod][N_3] is roughly comparable to that in [bmim][N_3].

D. Ionic conductivity

Ionic conductivity was calculated from NVT simulations using the Einstein relation:

$$\lambda = \lim_{t\to\infty} \lambda(t) = \lim_{t\to\infty} \frac{e^2}{6tVk_bT} \times \sum_{i,j}^{N} z_i z_j \langle([R_i(t) - R_i(0)])([R_j(t) - R_j(0)])\rangle, \quad (2)$$

where e is the electron charge, V is the volume of the simulation box, z_i and z_j are the charges over ions i and j in electrons, $\mathbf{R}_i(t)$ is the displacement of the ion i during time t, the summation is performed over all ions N in the simulation cell, and the brackets denote averaging over all ions and time origins. Conductivity can be decomposed into an "ideal" conductivity that would be realized if ion motion were uncorrelated, denoted λ_{uncorr}, and the degree to which ion motion is in fact uncorrelated, denoted α_d. The apparent degree of uncorrelated ion motion $\alpha_d(t)$ is given as the ratio of the apparent collective (total) charge transport $\lambda(t)$ to the apparent charge transport due to self-diffusion only $\lambda_{uncorr}(t)$, hence

$$\lambda_{uncorr} = \lim_{t\to\infty} \lambda_{uncorr}(t) = \lim_{t\to\infty} \frac{e^2}{6tVk_bT} \sum_{i}^{n} z_i^2 \langle[R_i(t) - R_i(0)]^2\rangle = \frac{e^2}{Vk_BT}(n_+ D_+^{app} + nD^{app}), \quad (3)$$

$$\alpha_d = \frac{\lambda}{\lambda_{uncor}} = \lim_{t\to\infty} \alpha_d(t) = \lim_{t\to\infty} \frac{\lambda(t)}{\lambda_{uncor}(t)}. \quad (4)$$

Here n_i is the number of ions of type i, with D_i^{app} the apparent self-diffusion coefficient of the associated ion type. Since Eq. (2) is a collective property of the system, calculation of the long-time limit of $\lambda(t)$ using Eq. (2) is challenging due to the poor statistics due to long time correlations which may be encountered while calculating a single collective property. While calculation of λ_{uncorr} benefits from the averaged nature of the calculation of the ion self-diffusion function, α_d remains a collective property. However, in casting the conductivity as a product of a non-correlated diffusive process with a correlated (dis)association process, we shift the time scale of the collective property from something that necessarily must be long enough to calculate the diffusion of correlated particles to one which only requires sufficient sampling over the relaxation time required for ion-ion correlations.

Due to the heavy screening present in ionic liquid systems, this is roughly equivalent with the time required for one to a few local cage relaxation events to occur, since once an ion is no longer a nearest (or second or third nearest) neighbor to its related counter-ion, it effectively quits feeling the effect of that counter-ion. Thus, if we calculate α_d for time scales corresponding to a few local-cage relaxation times, we can approximate α_d with a reasonable amount of statistical surety, as has been demonstrated in previous work.[3,4,19] Additional discussion of α_d is available in the supplemental information. For the systems investigated here, the degree of ion uncorrelated motion (α_d) was between 0.5 and 0.6, which is on the lower side of the typically observed α_d values 0.58–0.85 previously reported for 29 ILs (Ref. 3) indicating a tendency toward higher cation/anion coordination in the imidazolium azide ILs than in most of the others we have investigated. The range of α_d 0.52–0.76 was also reported in other simulations[3,4,20,21] and experiments.[22–24]

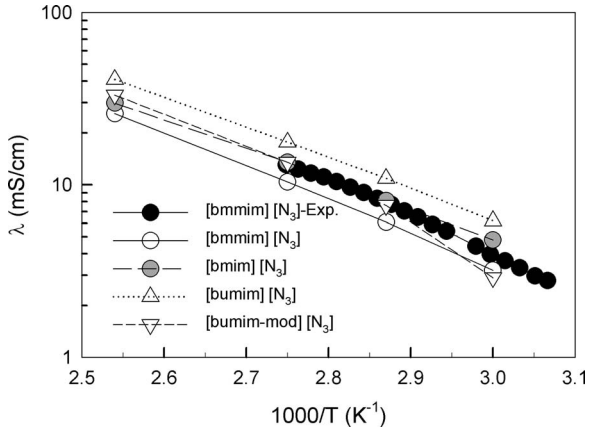

FIG. 5. Ionic conductivity as a function of temperature as obtained from MD simulations and experiment. Experimental data are taken from Ref. 17.

Ionic conductivities obtained from MD simulations are given in Figure 5 along with experimental data for [bmmim][N_3].[17] MD simulations employing the extended APPLE&P force field predict conductivity of [bmimm][N_3] as a function of temperature quite well, particularly when considering that other simulation attempts to quantify ion transport of imidazolium ILs have yielded dynamics[25,26] an order of magnitude slower than experiments. The dependence of IL ionic conductivity on cation shown in Figure 5 closely follows the order of self-diffusion coefficients. As with ion self-diffusion coefficients, increasing the dihedral barrier in the 2-butynyl group of bumim reduces dynamics about the same amount as replacing the butyl side chain with the smaller 2-butynyl increases them.

E. Rotational relaxation

The rotational relaxation times of our ions are defined first by choosing a basis for the cations with the x-axis along the C = C bond of the imidazolium ring, the y-axis perpendicular to the x-axis in the plane of the imidazolium ring, and the z-axis perpendicular to the plane of the imidazolium ring. The rotational autocorrelation function is defined by

$$P_1(t) = \langle \vec{e}_i(t) \cdot \vec{e}_i(0) \rangle , \quad (5)$$

with $\vec{e}_i(t)$ the unit vector represented by the i axis at time t. The innate time for the rotational relaxation is determined by fitting the autocorrelation function from time $t = 0$ to the time at which $P_1(t) = 0.01P_1(0)$ with a stretched exponential of the

Kohlrausch-Williams-Watts[27] form:

$$R_{KWW}(t) = A \exp\left(-\left(\frac{t}{\tau}\right)^{\beta}\right), \quad (6)$$

where A and β are fit parameters, t is time, and τ is the innate rotational relaxation decay time. Figure 6 presents the resultant time constants as a function of temperature for every axis of each imidazolium based cation, as well as the relaxation of the single linear axis for the azide anion. Rotations along the x-axis (roughly the "long" axis in the plane of the imidazolium ring) of the cations are very similar at all but the lowest temperature, with a slightly faster rotation rate for the [bumim] than the other cations, in line with expected projections of the volume of the ion along the indicated axis. Rotations along the other in plane axis fall out in order of the molecular volume, with the exception of the [bumim-mod] cation, which shows a decay rate more akin to the significantly bulkier [bmmim] cation. For rotation in the plane of the imidazolium ring, the relative rates of the unmodified cations are similar, with the [bumim-mod] cation falling between [bmim] and the slower [bmmim] ion. For the azide anion, the rotation time for the azide coupled with the [bmmim] is significantly faster than when associated with the remaining cations.

F. Enthalpy of vaporization

We calculate the enthalpy of vaporization using the following equation:

$$\Delta H_{VAP} = [U_{gas} - U_{liquid}] + RT, \quad (7)$$

where U_{gas} is the average molar energy of the ion pair in gas state at temperature T, U_{liquid} is the average molar energy of the ionic liquid in the liquid state at temperature T, and R is the universal gas constant. Enthalpies of vaporization obtained from MD simulations are summarized in Table II. Replacing hydrogen with CH_3 group on the central carbon "C-2" of the heterocyclic ring lowers ΔH_{VAP} by ~12 kJ/mol, while substitution of the butyl tail with 2-butynyl group increased enthalpy of vaporization by ~3 kJ/mol. It can be observed that the enthalpy of vaporization increases as the volume of the cation decreases, as indicated in Table II. Hence, ion diffusion and heat of vaporization seem to exhibit a counter-intuitive correlation, with the highest ion mobility being found in the IL with the highest heat of vaporization and hence strongest intermolecular interactions.

G. Intermolecular structure

Anion-anion center-of-mass radial distribution functions (RDFs) for the three ILs are shown in Figure 7. Cation-anion and cation-cation RDFs are given in the Supplementary Material.[28] The largest influence of changing the cation structure is seen in the anion-anion RDF, where the [bmmim][N_3] exhibits a significantly sharper peak than observed in [bmim][N_3] or [bumim][N_3]. 3-D isodensity distributions of the azide anions around the three cations are shown in Figure 8. The molecule at the center of distributions represents the average configuration of a bmmim cation.

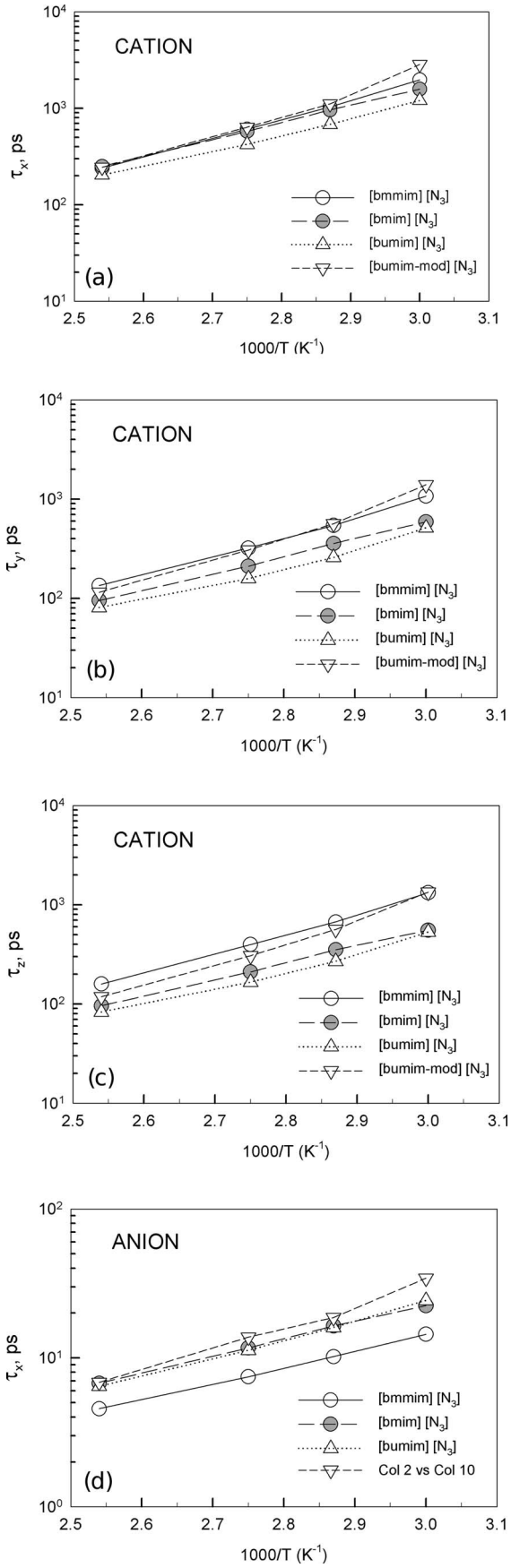

FIG. 6. Innate rotational relaxation time constants (τ) for the modified imidazolium cations along the C = C x-axis (a), in the imidazolium ring plane perpindicular to the C = C axis (b), and perpendicular to the imidazolium ring plane (c), as well as for the single azide axis (d).

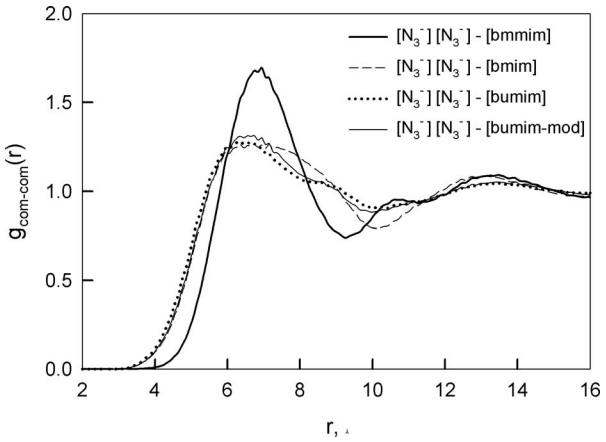

FIG. 7. Anion-anion center-of-mass radial distribution functions at 333 K.

The other two cations are omitted for clarity as these would largely overlap the displayed cation. The anion density isosurfaces are presented for half of each symmetric isosurface, with the plane of symmetry being the plane of the imidazolium ring. The surfaces are then plotted from both a "front" and "back" orientation to better visualize the surfaces. As can be seen, when the "'C-2" hydrogen is replaced by a CH_3 group, azide interaction with positively charged imidazolium is shifted from the central position of the "C-2" carbon (top of the ring) to the side of the ring away from the butyl side chain and to the faces of the ring. The interaction of the azide anion with the acidic hydrogen of the [bmim] cation is localized and shifted away from the methyl group on the ring toward to the butyl chain due to steric repulsion of the methyl group. However, interaction of azide anion with the [bumim] cation is shifted toward the methyl group. The preferred position of the butynyl group is in the *cis* conformation. Therefore, steric repulsion from the butynyl group becomes substantial pushing the azide anion back toward the methyl group on the ring.

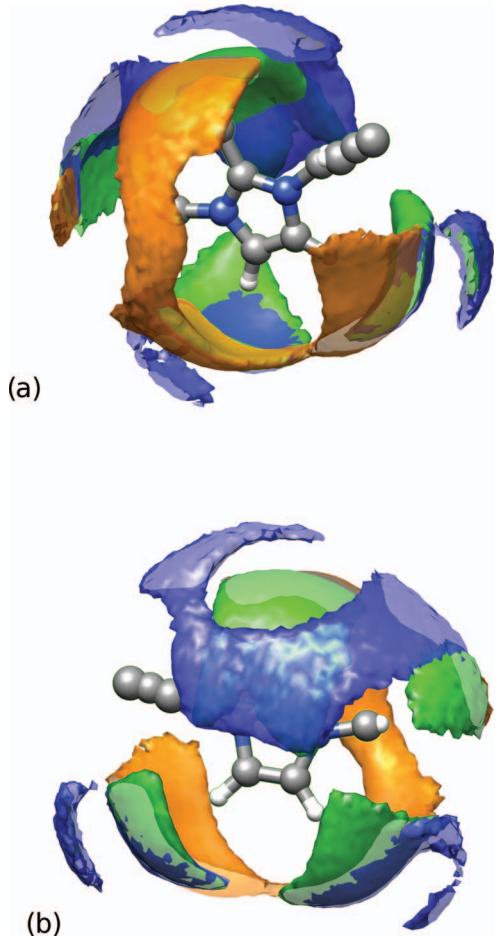

FIG. 8. Three-dimensional azide anion isosurfaces indicating regions with five times the bulk average azide nitrogen atom density around a cation. Blue isosurfaces corresponds to the position of azide around bmmim, green isosurfaces indicates the position of azide around bmim, and orange color isosurfaces represents the position of azide around bumim.

The lower ion diffusion rate in [bmmim][N_3] may be in part due to stronger ordering of azide anions illustrated by Figures 7 and 8. In particular, it appears relatively difficult for an azide ion to move from one face of the cation ring to the other over the top of the molecule in [bmmim][N_3] due to the presence of the "C-2" methyl substitution, as observed in simulations of other bmim-based ILs.[3]

Finally, the calculated x-ray structure factor for all three ILs can be found in the Supplementary Material.[28] These results are the first available (from experiment or simulation) x-ray structure factors for the studied ILs.

ACKNOWLEDGMENTS

The authors gratefully acknowledge financial support of this work by Air Force Office of Scientific Research, Department of the Air Force Contract No. FA9550-09-C-0110 to Wasatch Molecular Inc. An allocation of computer time from the Center for High Performance Computing at the University of Utah is also gratefully acknowledged.

[1]Y. H. Joo, H. X. Gao, Y. Q. Zhang, and J. M. Shreeve, Inorg. Chem. **49**, 3282 (2010).
[2]S. D. Chambreau, S. Schneider, M. Rosander, T. Hawkins, C. J. Gallegos, M. F. Pastewait, and G. L. Vaghjiani, J. Phys. Chem. A **112**, 7816 (2008).
[3]O. Borodin, J. Phys. Chem. B **113**, 11463 (2009).
[4]O. Borodin, W. Gorecki, G. D. Smith, and M. Armand, J. Phys. Chem. B **114**, 6786 (2010).
[5]G. D. Smith, O. Borodin, L. Li, H. Kim, Q. Liu, J. E. Bara, D. L. Gin, and R. Nobel, Phys. Chem. Chem. Phys. **10**, 6301 (2008).
[6]O. Borodin, G. D. Smith, and H. Kim, J. Phys. Chem. B **113**, 4771 (2009).
[7]M. J. Frisch, G. W. Trucks, H. B. Schlegel *et al.*, GAUSSIAN 09, Revision A.02, Gaussian, Inc., Wallingford, CT, 2009.
[8]A. Lee, C. K. Law, and A. Makino, Combust. Flame **78**, 263 (1989).
[9]For information on obtaining the APPLE&P forcefield please see http://www.wasatchmolecular.com.
[10]The Lucretius molecular dynamics simulation package is available free of charge. For information, please contact info@wasatchmolecular.com.
[11]B. J. Palmer, J. Comput. Phys. **104**, 470 (1993).
[12]B. T. Thole, Chem. Phys. **59**, 341 (1981).
[13]G. J. Martyna, D. J. Tobias, and M. L. Klein, J. Chem. Phys. **101**, 4177 (1994).
[14]O. Borodin, G. D. Smith, T. D. Sewell, and D. Bedrov, J. Phys. Chem. B **112**, 734 (2008).
[15]T. D. Sewell, R. Menikoff, D. Bedrov, G. D. Smith, J. Chem. Phys. **119**, 7417 (2003).
[16]S. Schneider, T. Hawkins, M. Rosander, J. Mills, G. Vaghjiani, and S. Chambreau, Inorg. Chem. **47**, 6082 (2008).
[17]Y. O. Andriyko, W. Reischl, and G. E. Nauer, J. Chem. Eng. Data **54**, 855 (2009).
[18]B. Dunweg and K. Kremer, J. Chem. Phys. **99**, 6983 (1993).
[19]O. Borodin and G. D. Smith, J. Phys. Chem. B **110**, 11481 (2006).
[20]W. Zhao, F. Leroy, B. Heggen, S. Zahn, B. Kirchner, S. Balasubramanian, and F. Muller-Plathe, J. Am. Chem. Soc. **131**, 15825 (2009).

[21]C. Schroder and O. Steinhauser, J. Chem. Phys. **131**, 114504 (2009).
[22]H. Tokuda, K. Hayamizu, K. Ishii, M. Abu Bin Hasan Susan, and M. Watanabe, J. Phys. Chem. B **108**, 16593 (2004).
[23]H. Tokuda, K. Hayamizu, K. Ishii, M. Abu Bin Hasan Susan, and M. Watanabe, J. Phys. Chem. B **109**, 6103 (2005).
[24]H. Tokuda, K. Ishii, M. Abu Bin Hasan Susan, S. Tsuzuki, K. Hayamizu, and M. Watanabe, J. Phys. Chem. B **110**, 2833 (2006).
[25]S. Tsuzuki, W. Shinoda, H. Saito, M. Mikami, H. Tokuda, and M. Watanabe, J. Phys. Chem. B **113**, 10641 (2009).
[26]T. Koddermann, D. Paschek, and R. Ludwig, Chem. Phys. Chem. **8**, 2464 (2007).
[27]G. Williams and D. C. Watts, Trans. Far. Soc. **66**, 80 (1970).
[28]See supplementary material at http://dx.doi.org/10.1063/1.4718800 for cation/anion and cation/cation radial distribution functions as well as X-Ray weighted structure factors.